This PDF file includes:

Supplementary Text
Figures and captions S1-S4
Captions for Tables S1-S2
Supplementary references

S1. Data set compilation

All data compiled are provided in an Excel file, with one sheet per site or paper (Table S1) for a total of 3895 data points across 79 sites or papers. The compiled sites are:

1 - Sao Pedro de Moel, Portugal, Late Sinemurian–Lower Pliensbachian (Plancq et al., 2016)

2 - Peniche, Portugal, Early Pliensbachian (Mattioli, unpublished data)

3 - Peniche, Portugal, Late Pliensbachian (Reggiani et al., 2010)

4 - La Cerradura, Spain, Late Pliensbachian–Early Toarcian (Reolid et al., 2014)

5 - Peniche, Portugal, Early Toarcian (Mattioli et al., 2009; Suan et al., 2008)

6 - Tournadous, France, Late Pliensbachian–Early Toarcian (Mailliot et al., 2009; Suan et al., 2008)

7 - Saint-Paul-des-Fonts, France, Late Pliensbachian–Early Toarcian (Mailliot et al., 2009; Suan et al., 2008)

8 - Somma, Italy, Late Pliensbachian–Early Toarcian (Mattioli et al., 2009)

9 - Dotternhausen, Germany, Early Toarcian (Mattioli et al., 2009)

10 - Yorkshire, UK, Early Toarcian (Plancq, 2009)

11 - Réka Valley, Hungary, Early Toarcian (Plancq, 2009)

12 - Chionistra, Greece, Early Toarcian (Kafousia et al., 2014)

13 - HTM-102, France, Early Toarcian (Mattioli et al., 2009)

14 - K2-5, France, Early Toarcian (Plancq, 2009)

15 - Rabaçal, Portugal, Late Pliensbachian–Late Toarcian (Kenjo, 2010)

16 - Cabo Mondego, Portugal, Late Aalenian–Early Bajocian (Suchéras-Marx et al., 2013; Suchéras-Marx et al., 2012)

17 - Chaudon-Norante, France, Late Aalenian–Early Bajocian (Suchéras-Marx et al., 2013; Suchéras-Marx et al., 2014)

18 - La Voulte, France, Middle Callovian–Early Oxfordian (Giraud, unpublished data)

19 - La Voulte, France, Middle Oxfordian (Excoffier, 2001; Pittet, 2006)

20 - Meussia, France, Middle Oxfordian (Excoffier, 2001; Pittet, 2006)

21 - Balingen–Tieringen, Germany, Late Oxfordian (Mattioli, unpublished data; Pittet, 2006)

22 - Plettenberg, Germany, Late Oxfordian (Olivier et al., 2004; Pittet, 2006)

23 - Le Pas de l'Assassin, France, Late Oxfordian–Early Kimmeridgian (Carcel, 2009; Carcel et al., 2010)

24 - DSDP105, North Atlantic, Tithonian–Valanginian (Bornemann et al., 2003)

25 - DSDP534A, North Atlantic, Tithonian–Valanginian (Bornemann et al., 2003)

26 - DSDP367, North Atlantic, Tithonian–Valanginian (Bornemann et al., 2003; Lancelot and Seibold, 1978)

27 - Perisphinctes Ravine, Greenland, Late Ryazanian–Late Hauterivian (Pauly et al., 2012)

28 - Rødryggen, Greenland, Late Ryazanian–Late Hauterivian (Pauly et al., 2012)

29 - Polaveno, Italy, Late Berriasian–Early Hauterivian (Erba and Tremolada, 2004; Gréselle and Pittet, 2010)

30 - DSDP534A, North Atlantic, Late Berriasian–Early Hauterivian (Bornemann et al., 2005; Gréselle and Pittet, 2010)

31 - DSDP603B, North Atlantic, Late Berriasian–Late Valanginian (Bornemann et al., 2005; Gréselle and Pittet, 2010)

32 - Vergol–La Charce, France, Valanginian (Gréselle and Pittet, 2010; Gréselle et al., 2011)

33 - Carajuan, France, Early Valanginian (Gréselle and Pittet, 2010; Riquier, 2002)

34 - DSDP535, Mexico Gulf, Early Valanginian–Early Hauterivian (Kessels et al., 2006)

35 - ODP638, North Atlantic, Early Valanginian–Early Hauterivian (Kessels et al., 2006)

36 - BGS81/43, North Atlantic, Early Valanginian–Early Hauterivian (Kessels et al., 2006)

37 - BGS81/43, North Sea, Late Valanginian–Late Hauterivian (Williams and Bralower, 1995)

38 - Speeton, UK, Early Hauterivian–Barremian (Williams and Bralower, 1995)

39 - Otto Gott, Germany, Barremian (Mutterlose, 1998; Williams and Bralower, 1995)

40 - Nora-1, Danemark, Barremian (Mutterlose and Bottini, 2013)

41 - North Jens-1, Danemark, Late Barremian–Early Aptian (Mutterlose and Bottini, 2013)

42 - A39-Braunschweig, Germany, Early Barremian–Early Aptian (Pauly et al., 2013)

43 - Takal Kuh, Iran, Early Aptian (Mahanipour et al., 2011)

44 - Notre-Dame-de-Rosans, France, Aptian (Giraud et al., 2018)

45 - Pré-Guittard, France, Late Aptian (Herrle, 2002; Herrle et al., 2003)

46 - Alma, Morocco, Late Aptian–Early Albian (Peybernes et al., 2013)

47 - Addar, Morocco, Late Aptian–Early Albian (Peybernes et al., 2013)

48 - Tamzergout, Morocco, Late Aptian–Early Albian (Peybernes et al., 2013)

49 - Hyèges, France, Late Aptian (Giraud, unpublished data; Herrle, 2002)

50 - L'Arboudeysse, France, Early Albian (Herrle, 2002)

51 - DSDP545, North Atlantic, Early Albian (Herrle, 2002)

52 - Col de Palluel, France, Late Albian (Bornemann et al., 2005)

53 - Blieux, France, Early Cenomanian–Middle Cenomanian (Giraud et al., 2013; Reboulet et al., 2013)

54 - Wunstorf, Germany, Middle Cenomanian–Middle Turonian (Linnert et al., 2010; Voigt et al., 2008)

55 - ODP1258, Central Atlantic, Early Cenomanian–Middle Turonian (Hardas and Mutterlose, 2007; Shipboard Scientific Party, 1985)

56 - ODP1260, Central Atlantic, Early Cenomanian–Early Turonian (Hardas and Mutterlose, 2007; Shipboard Scientific Party, 1985)

57 - Holywell Pinnacles, UK, Late Cenomanian–Early Turonian (Linnert et al., 2011b; Voigt et al., 2008)

58 - DSDP549-551, North Atlantic, Middle Cenomanian–Late Maastrichtian (Linnert et al., 2011a; Shipboard Scientific Party, 1985)

59 - Kronsmoor, Germany, Late Campanian–Early Maastrichtian (Linnert et al., 2016)

60 - Qreiya 1, Egypt, Danian–Selandian (Youssef Ali, 2009)

61 - Qreiya 3, Egypt, Danian–Selandian (Sprong et al., 2011)

62 - Araas, Egypt, Danian (Youssef Ali, 2009)

63 - Duwi, Egypt, Danian (Youssef Ali, 2009)

64 - ODP1260B, Central Atlantic, Late Paleocene–Early Eocene (Mutterlose et al., 2007; Youssef Ali and Mutterlose, 2004)

65 - Wadi Abu Ghurra, Egypt, Late Maastrichtian–Early Eocene (Youssef Ali and Mutterlose, 2004)

66 - Kurkur Naqb Dungul, Egypt, Late Paleocene–Early Eocene (Youssef Ali and Mutterlose, 2004)

67 - ODP1263, South Atlantic, Late Paleocene–Early Eocene (Zuzlewski, 2014)

68 - ODP1209A, North Pacific, Eocene (Salaviale, 2013)

69 - DSDP511, South Atlantic, Rupelian–Priabonian (Plancq et al., 2014)

70 - DSDP516, South Atlantic, Oligocene–Miocene (Plancq et al., 2012; Plancq et al., 2013)

71 - DSDP608, North Atlantic, Oligocene–Miocene (Plancq et al., 2013)

72 - DSDP588C, North Atlantic, Oligocene–Miocene (Plancq et al., 2013)

73 - ODP752A, Indian Ocean, Miocene–Pleistocene (Suchéras-Marx and Henderiks, 2012)

74 - DSDP525, South Atlantic, Miocene–Pleistocene (Suchéras-Marx and Henderiks, 2012)

75 - ODP806B, East Pacific, Miocene–Pleistocene (Suchéras-Marx and Henderiks, 2012)

76 - ODP707A, Indian Ocean, Miocene–Pleistocene (Suchéras-Marx and Henderiks, 2012)

77 - ODP982B, North Atlantic, Miocene–Pleistocene (Suchéras-Marx and Henderiks, 2012)

78 - Punta di Maiata, Italy, Zanclean (Mattioli, unpublished data)

79 - Punta Grande/Punta Piccola, Italy, Pliocene (Plancq et al., 2015)

S2. Impact of LOESS smoothing factor on the long-term trend of nannofossil accumulation rate. Interpretation of the long-term trend can be arguably linked to the smoothing factor (SF) selected for the LOESS (LOcally wEighted Scatterplot Smoothing). In Fig. S1 we present the nannofossil accumulation rate for SF = 0.1, 0.25, 0.5, 0.75, and 1. The smaller the smoothing factor, the rougher and less marked the smoothing is. Whereas the smoothed curve at SF 0.1 is clearly influenced by the sampling resolution along the analyzed time series, from SF 0.25 to SF 1 the same long-term trend is observed without short-term artifact. Accordingly, the discussed trend appears to be a reliable long-term pattern unrelated to the selected SF-value.

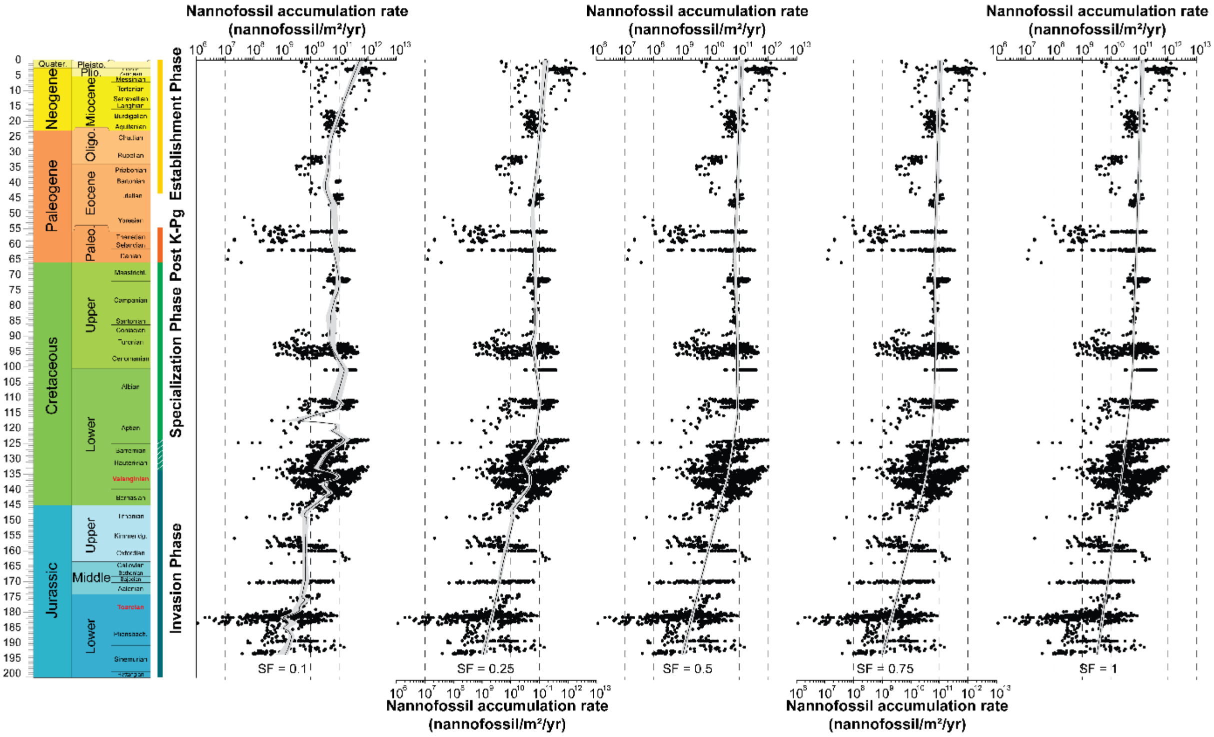

Fig. S1. Comparison of the LOESS smoothing for nannofossil accumulation rates (nannofossil/m²/yr) with five different smoothing factor values (from left to right): SF 0.1, SF 0.25, SF 0.5, SF 0.75, and SF 1. SF 0.5 is the one discussed in the main text.

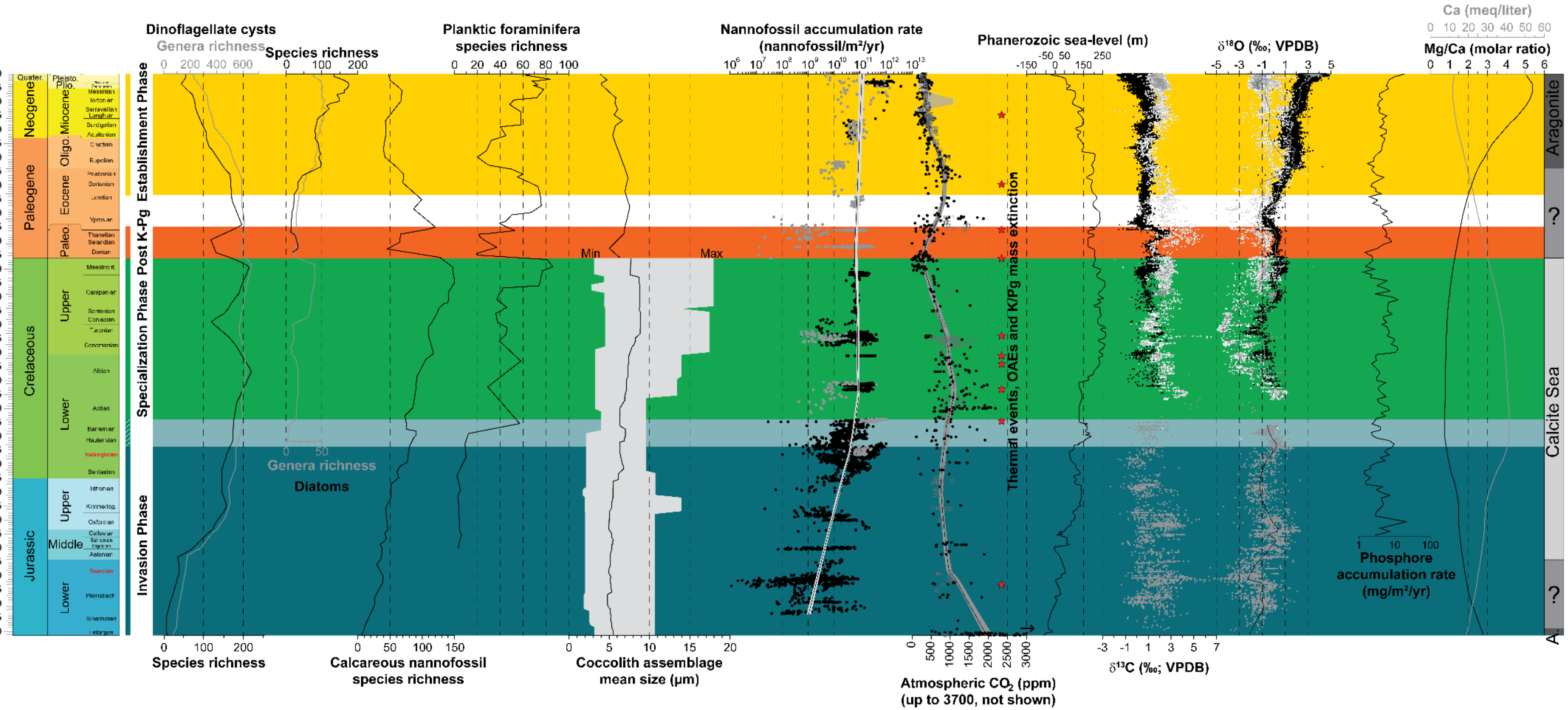
Dinoflagellate cysts
Genera richness
Species richness
Planktic foraminifera species richness
Nannofossil accumulation rate (nannofossil/m²/yr)
Phanerozoic sea-level (m)
δ18O (‰; VPDB)
Ca (meq/liter)
Mg/Ca (molar ratio)
Neogene
Paleogene
Cretaceous
Jurassic
Establishment Phase
Post K-Pg
Specialization Phase
Invasion Phase
Min
Max
Genera richness
Diatoms
Thermal events, OAEs and K/Pg mass extinction
Phosphore accumulation rate (mg/m²/yr)
Aragonite
Calcite Sea
Species richness
Calcareous nannofossil species richness
Coccolith assemblage mean size (µm)
Atmospheric CO2 (ppm) (up to 3700, not shown)
δ13C (‰; VPDB)

Fig. S2. Comparison of microplankton evolution and environmental/climatic changes through time. Dinoflagellate cyst richness (number of species in black and genera in grey) (Kooistra et al., 2007; Stover et al., 1996); diatoms richness (number of species in black and genera in grey) (Spencer-Cervato, 1999), nannoplankton species richness (Bown, 2005); planktic foraminifera species richness (Peters et al., 2013); coccolith mean size at the assemblage level (µm, Mesozoic (Aubry et al., 2005) and Cenozoic (Herrmann and Thierstein, 2012)); nannofossil accumulation rate (this study); atmospheric CO_2 (ppm) (Foster et al., 2017; Mejía et al., 2017); compilation of OAEs, thermal events and K/Pg mass extinction; Phanerozoic sea-level (m) (Hardenbol et al., 1998); $\delta^{13}C$ (‰, VPDB; square: belemnite; open circle: planktic foraminifera; black circle: benthic foraminifera) (Friedrich et al., 2005; Prokoph et al., 2008); $\delta^{18}O$ (‰, VPDB; square: belemnite; open circle: planktic foraminifera; black circle: benthic foraminifera) (Friedrich et al., 2005; Prokoph et al., 2008); phosphorus accumulation rate (mg/m²/yr) (Föllmi, 1995); Mg/Ca (molar ratio), Ca (mEq/L), calcite vs. aragonite seas (Stanley, 2008). The dinoflagellate species richness presents the same broad pattern as calcareous nannofossil species richness with an increase up to the Early Cretaceous and a decrease from the end of the Paleocene up to Holocene (Falkowski et al., 2004). This long-term pattern is interrupted by a two-phase decrease: one during the early Late Cretaceous and another during the K/Pg crisis. The long-term variations of diatoms species and genera richness are completely different from those observed for both calcareous nannofossils and dinoflagellates cysts. Unfortunately, the lack of literature data on diatoms and dinoflagellate accumulation rates hampers further comparisons with the evolutionary pattern discussed for calcareous nannoplankton. The record of $\delta^{13}C$ and phosphorus accumulation rates is not discussed in the main text. They do not show long-term changes, but rather shorter cyclic variations intimately related to climate changes which are tuned by orbital cycles. On the long-term scale, there is no relationship between calcareous nannoplankton evolution and $\delta^{13}C$ or phosphorus accumulation rates, but there are likely relationships on the short-term scale (e.g. Mattioli et al., 2009) which are not captured in the present record.

S3. Disparity of sampling through time and space. The database presented in this study gathered 3895 samples from 79 sites over the last 193 Myr. This large amount of data is not evenly distributed through time. Figure S3 presents the number of sample per Myr and the number of sites per Myr. Usually, the more sites compiled, the more samples there are in the database, although this is not observed for the Neogene. This figure also highlights the discrete sampling pattern, with some time intervals being more densely studied than others. Three time-intervals are highly documented: the early Toarcian (Early Jurassic), the Valanginian (Early Cretaceous), and the Cenomanian/Turonian transition (Late Cretaceous). To a lesser extent, we can also cite the Aptian-Albian transition (Early Cretaceous) and the Paleogene.

The maps in Fig. S3 present the sites studied for the four geological Periods considered (Quaternary excluded). The Jurassic samples are mainly represented by European sites and are all located in the Northern Hemisphere. The Cretaceous samples are equably distributed between European and Atlantic deep-sea drilling sites, all of them being from the Northern Hemisphere. The Paleogene samples are from Egyptian sites and four deep-sea drilling sites, three from the Central-South Atlantic and one from the North Pacific. Finally, the Neogene samples are dominated by deep-sea drilling sites from the Southern Hemisphere. The analyzed database is not uniform through time, with a shift from European and Northern Hemisphere Mesozoic sites to Southern Hemisphere samples in the Neogene.

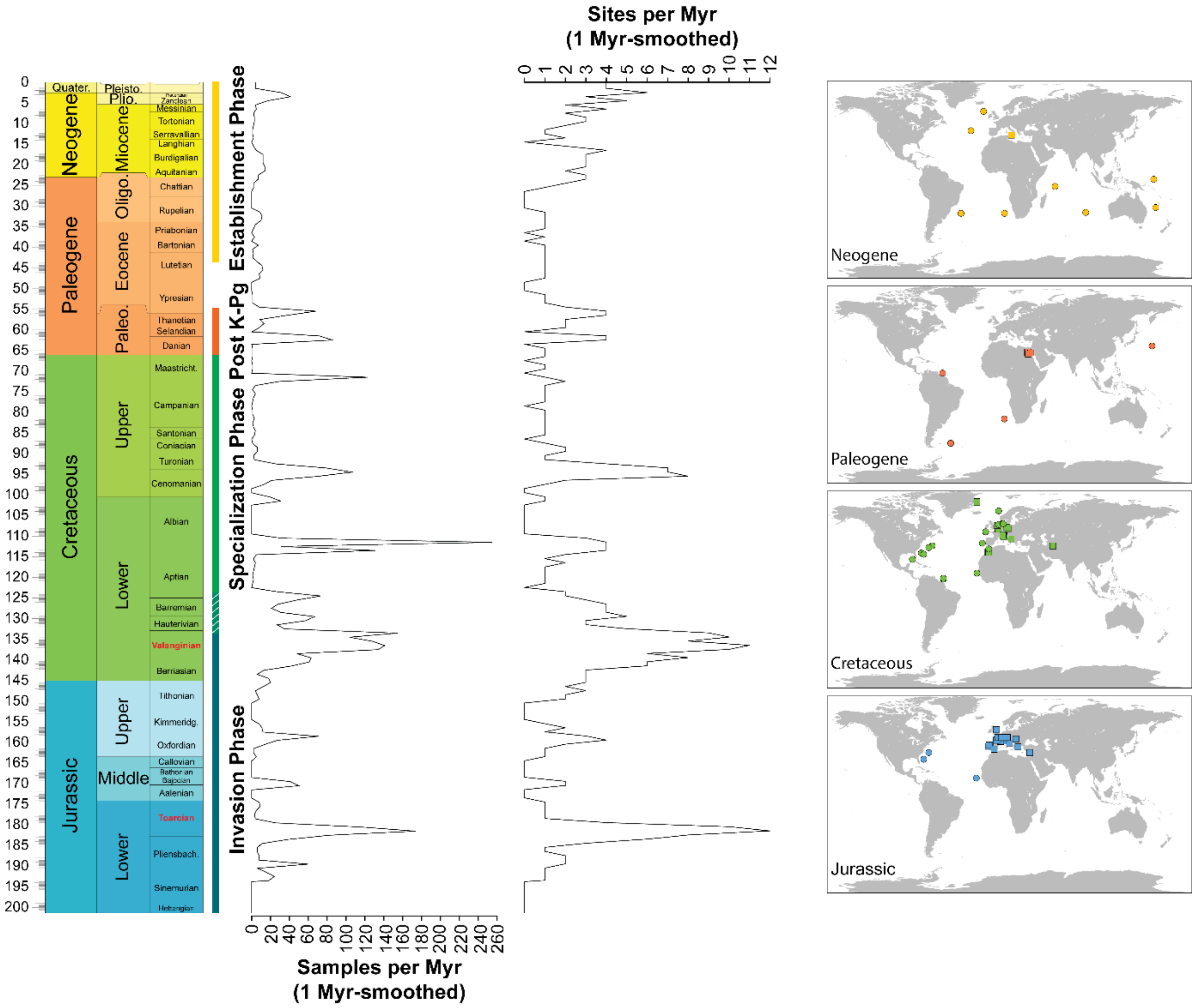

Fig. S3. Number of samples and sites per Myr and sites location for the four Periods studied.

S4. Impact of sedimentary rates on the computation of nannofossil accumulation rate. This study discusses nannofossil accumulation rate which is derived from nannofossil absolute abundance and sedimentary rates (see Methods). All absolute abundance data compiled but one paper (Erba and Tremolada, 2004) have been obtained using the same method; methodological biases are thus negligible at this level. Conversely, the sedimentary rates used to calculate nannofossil accumulation rates derive from the International Chronostratigraphic Chart 2012 (Gradstein et al., 2012) or from cyclostratigraphy-based estimated durations. These two different methods used to calculate nannofossil accumulation rates might impact the short-term fluctuations observed, but they are not likely to affect the long-term trends discussed here. Figure S4 compares the long-term trends (LOESS SF 0.5) for nannofossil absolute abundance (nannofossil/g_{bulk}) and nannofossil accumulation rate (nannofossil/m^2/yr). The comparison of these two plots highlights some differences due to local sedimentary patterns influencing the nannofossil accumulation rate (e.g., during the Early Cretaceous); nevertheless, the overall long-term trend discussed in the article is the same between nannofossil absolute abundance and accumulation rate. This observation allows us to rule out a bias effect of sedimentary rate calculation on the resulting long-term trend.

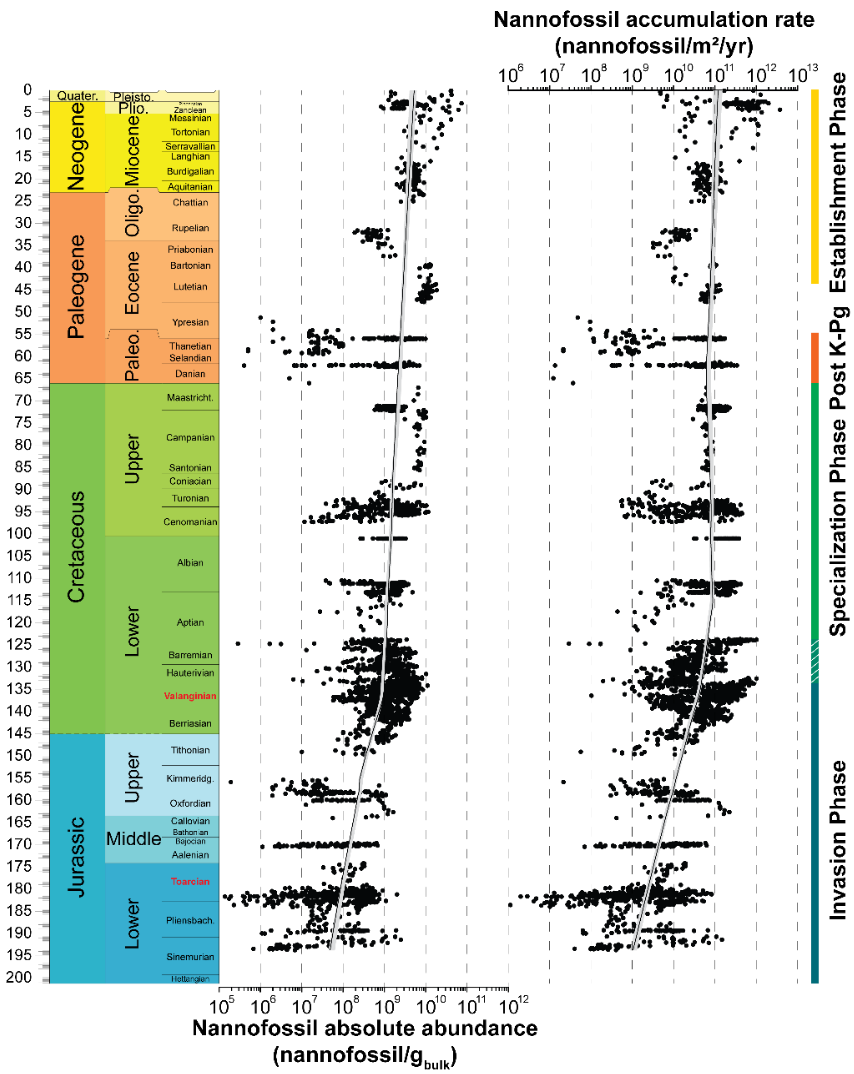

Fig. S4. Comparison between the compiled nannofossil absolute abundances (nannofossil/g_{bulk}) and nannofossil accumulation rates (nannofossil/m^2/yr) computed in this study.

Table S1. Dataset of nannofossil accumulation rate in the different settings studied in this work, sorted in chronological order. Each sheet presents the location of the site, the age (relative and absolute), the nannofossil absolute abundance, the sedimentation rate, the nannofossil accumulation rate, and other information such as the sample name, height in the section and the published reference.

Table S2. Dataset of nannofossil accumulation rate used to construct Fig. 3. The table presents for both considered geological stages (i.e., Toarcian and Valanginian) the location of each site, their mean nannofossil absolute abundance and mean nannofossil accumulation rate, and the number of sample per site.

S5. Supplementary references for nannofossil absolute abundance, nannofossil accumulation rate and sedimentation rate calculation compiled in this study, and supplementary references in Fig. S2 (by alphabetical order)

Bornemann, A., Aschwer, U., and Mutterlose, J.: The impact of calcareous nannofossils on the pelagic carbonate accumulation across the Jurassic-Cretaceous boundary, Palaeogeogr. Palaeoclimatol. Palaeoecol., 199, 187-228, 2003.

Bornemann, A., and Mutterlose, J.: Calcareous nannofossil and d13C records from the early Cretaceous of the western Atlantic ocean: evidence for enhanced fertilization across the Berriasian-Valanginian transition, Palaios, 23, 821-832, 2008.

Bornemann, A., Pross, J., Reichelt, K., Herrle, J. O., Hemleben, C., and Mutterlose, J.: Reconstruction of short-term palaeoceanographic changes during the formation of the Late Albian 'Niveau Breistroffer' black shales (Oceanic Anoxic Event 1d, SE France), J. Geol. Soc. London, 162, 623-639, http://dx.doi.org/10.1144/0016-764903-171, 2005.

Carcel, D.: Caractérisation des environnements de dépôt dominés par les tempêtes, PhD, Université Claude Bernard Lyon1, 131 pp., 2009.

Carcel, D., Colombié, C., Giraud, F., and Courtinat, B.: Tectonic and eustatic control on a mixed siliciclastic-carbonate platform during the Late Oxfordian-Kimmeridgian (La Rochelle platform, western France), Sediment. Geol., 223, 334-359, 2010.

Excoffier, F. : Modèle d'interaction climat–niveau marin et le signal carbonate dans les sédiments hémipélagiques du Mésozoïque (Oxfordien, Valanginien, SE France), Master Thesis, Université Claude Bernard Lyon1, 42 pp., 2001.

Föllmi, K. B.: 160 m.y. record of marine sedimentary phosphorus burial: Coupling of climate and continental weathering under greenhouse and icehouse conditions, Geology, 23, 859-862, 1995.

Friedrich, O., Herrle, J. O., and Hemleben, C.: Climatic changes in the Late Campanian-Early Maastrichian: Micropaleontological and stable isotopic evidence from an epicontinental sea, J. Foraminifer. Res., 35, 228-247, http://dx.doi.org/10.2113/35.3.228, 2005.

Friedrich, O., Norris, R. D., and Erbacher, J.: Evolution of middle to Late Cretaceous oceans-A 55 m.y. record of Earth's temperature and carbon cycle, Geology, 40, 107-110, 2012.

Giraud, F.: Unpublished data – La Voulte, France.

Giraud, F.: Unpublished data – Hyèges, France.

Giraud, F., Pittet, B., Grosheny, D., Baudin, F., Lécuyer, C., and Sakamoto, T.: The palaeoceanographic crisis of the Early Aptian (OAE 1a) in the Vocontian Basin (SE France), Palaeogeogr. Palaeoclimatol. Palaeoecol., https://doi.org/10.1016/j.palaeo.2018.09.014, 2018.

Giraud, F., Reboulet, S., Deconinck, J.-F., Martinez, M., Carpentier, A., and Bréziat, C.: The Mid-Cenomanian Event in southeastern France: Evidence from palaeontological and clay mineralogical data, Cretac. Res., 46, 43-58, 2013.

Gréselle, B., and Pittet, B.: Sea-level reconstructions from the Peri-Vocontian Zone (South-east France) point to Valanginian glacio-eustasy, Sedimentology, 57, 1640-1684, 2010.

Gréselle, B., Pittet, B., Mattioli, E., Joachimski, M., Barbarin, N., Riquier, L., Reboulet, S., and Pucéat, E.: The Valanginian isotope event: A complex suite of palaeoenvironmental perturbations, Palaeogeogr. Palaeoclimatol. Palaeoecol., 306, 41-57, 2011.

Hardas, P., and Mutterlose, J.: Calcareous nannofossil assemblages of Oceanic Anoxic Event 2 in the equatorial Atlantic: Evidence of an eutrophication event, Mar. Micropaleontol., 66, 52-69, 2007.

Hardenbol, J., Thierry, J., Farley, M. B., Jacquin, T., De Graciansky, P.-C., and BVail, P. R.: Mesozoic and Cenozoic sequence stratigraphy of European basins, SEPM Spec. Publ., 60, 1-13, 1998.

Herrle, J. O.: Paleoceanographic and Paleoclimatic Implications on Mid-Cretaceous Black Shale Formation in the Vocontian Basin and the Atlantic: Evidence from Calcareous Nannofossils and Stable Isotopes, Tubinger Mikropaläontologische Mitteilungen, 27, 144, 2002.

Herrle, J. O., Pross, J., Friedrich, O., and Hemleben, C.: Short-term environmental changes in the Cretaceous Tethyan Ocean: micropalaeontological evidence from the Early Albian Oceanic Anoxic Event 1b, Terra Nova, 15, 14-19, 2003.

Kafousia, N., Karakitsios, V., Mattioli, E., Kenjo, S., and Jenkyns, H. C.: The Toarcian Oceanic Anoxic Event in the Ionian Zone, Greece, Palaeogeogr. Palaeoclimatol. Palaeoecol., 393, 135-145, http://dx.doi.org/10.1016/j.palaeo.2013.11.013, 2014.

Kenjo, S.: Biostratigraphie à nannofossiles calcaires et changements paléoenvironnemantaux au Toarcien. L'exemple du Bassin Lusitanien (Portugal), Master Thesis, Université Claude Bernard Lyon1, 50 pp, 2010.

Kessels, K., Mutterlose, J., and Michalzik, D.: Early Cretaceous (Valanginian - Hauterivian) calcareous nannofossils and isotopes of the northern hemisphere: proxies for the understanding of Cretaceous climate, Lethaia, 39, 157-172, http://dx.doi.org/10.1080/00241160600763925, 2006.

Lancelot, Y., and Seibold, E.: The Evolution of the Central Northeastern Atlantic—Summary of Results of DSDP Leg 41, DSDP Reports and Publications XLI, 1215-1245, 1978.

Linnert, C., Engelke, J., Wilmsen, M., and Mutterlose, J.: The impact of the Maastrichtian cooling on the marine nutrient regime—Evidence from midlatitudinal calcareous nannofossils, Paleoceanography, 31, 2015PA002916, http://dx.doi.org/10.1002/2015PA002916, 2016.

Linnert, C., Mutterlose, J., and Erbacher, J.: Calcareous nannofossils of the Cenomanian/Turonian boundary interval from the Boreal Realm (Wunstorf, northwest Germany), Mar. Micropaleontol., 74, 38-58, 2010.

Linnert, C., Mutterlose, J., and Herrle, J. O.: Late Cretaceous (Cenomanian-Maastrichtian) calcareous nannofossils from Goban Spur (DSDP Sites 549, 551): Implications for the palaeoceanography of the proto North Atlantic, Palaeogeogr. Palaeoclimatol. Palaeoecol., 299, 507-528, 2011a.

Linnert, C., Mutterlose, J., and Mortimore, R.: Calcareous nannofossils from Eastbourne (Souteastern England) and the paleoceanography of the Cenomanian-Turonian boundary interval, Palaios, 26, 298-313, 10.2110/palo.2010.p10-130r, 2011b.

Mahanipour, A., Mutterlose, J., Kani, A. L., and Adabi, M. H.: Palaeoecology and biostratigraphy of early Cretaceous (Aptian) calcareous nannofossils and the $\delta^{13}C_{carb}$ isotope record from NE Iran, Cretac. Res., 32, 331-356, http://dx.doi.org/10.1016/j.cretres.2011.01.006, 2011.

Mailliot, S., Mattioli, E., Bartolini, A., Baudin, F., Pittet, B., and Guex, J.: Late Pliensbachian-Early Toarcian (Early Jurassic) environmental changes in an epicontinental basin of NW Europe (Causses area, central France): A micropaleontological and geochemical approach, Palaeogeogr. Palaeoclimatol. Palaeoecol., 273, 346-364, 2009.

Mattioli, E.: Unpublished data – Balingen–Tieringen, Germany.

Mattioli, E.: Unpublished data – Peniche, Portugal.

Mattioli, E.: Unpublished data – Punta de Maiata, Italy.

Mattioli, E., Pittet, B., Petitpierre, L., and Mailliot, S.: Dramatic decrease of pelagic carbonate production by nannoplankton across the Early Toarcian anoxic event (T-OAE), Glob. Planet. Change, 65, 134-145, 2009.

Mutterlose, J.: The Lower and Upper Cretaceous of the Hannover-Braun-schweig area (NW Germany), in: Key localities of the Northwest European Cretaceous, edited by: Mutterlose, J., Bornemann, A., Rauer, S., Spaeth, C., and Wood, C. J., Bochumer geologische und geotechnische Arbeiten, Bochum, 81-90, 1998.

Mutterlose, J., and Bottini, C.: Early Cretaceous chalks from the North Sea giving evidence for global change, Nat. Commun., 4, 1686, http://dx.doi.org/10.1038/ncomms2698, 2013.

Mutterlose, J., Linnert, C., and Norris, R.: Calcareous nannofossils from the Paleocene-Eocene Thermal Maximum of the equatorial Atlantic (ODP Site 1260B): Evidence for tropical warming, Mar. Micropaleontol., 65, 13-31, 2007.

Olivier, N., Pittet, B., and Mattioli, E.: Palaeoenvironmental control on sponge-microbialite reefs and contemporaneous deep-shelf marl-limestone deposition (Late Oxfordian, southern Germany), Palaeogeogr. Palaeoclimatol. Palaeoecol., 212, 233-263, 2004.

Pauly, S., Mutterlose, J., and Alsen, P.: Early Cretaceous palaeoceanography of the Greenland-Norwegian Seaway evidenced by calcareous nannofossils, Mar. Micropaleontol., 90-91, 72-85, 2012.

Pauly, S., Mutterlose, J., and Wray, D. S.: Palaeoceanography of Lower Cretaceous (Barremian-Lower Aptian) black shales from northwest Germany evidenced by calcareous nannofossils and geochemistry, Cretac. Res., 42, 28-43, http://dx.doi.org/10.1016/j.cretres.2013.01.001, 2013.

Peters, S. E., Kelly, D. C., and Fraass, A. J.: Oceanographic controls on the diversity and extinction of planktonic foraminifera, Nature, 493, 398-403, 2013.

Peybernes, C., Giraud, F., Jaillard, E., Robert, E., Masrour, M., Aoutem, M., and Içame, N.: Stratigraphic framework and calcareous nannofossil productivity of the Essaouira-Agadir

Basin (Morocco) during the Aptian-Early Albian: Comparison with the north-Tethyan margin, Cretac. Res., 39, 149-169, 2013.

Pittet, B.: Les alternances marno–calcaires ou l'enregistrement de la dynamique de production et d'export des plates–formes carbonatées, HDR Thesis, Université Claude Bernard Lyon1, 79 pp, 2006.

Plancq, J.: Caractéristiques de la phase de récupération par le nannoplancton calcaire après l'événement anoxique du Toarcien inférieur (Jurassique inférieur), Master Thesis, Université Claude Bernard Lyon1, 50 pp., 2009.

Plancq, J., Grossi, V., Henderiks, J., Simon, L., and Mattioli, E.: Alkenone producers during late Oligocene-early Miocene revisited, Paleoceanography, 27, PA1202, 2012.

Plancq, J., Grossi, V., Pittet, B., Huguet, C., Rosell-Melé, A., and Mattioli, E.: Multi-proxy constraints on sapropel formation during the late Pliocene of central Mediterranean (southwest Sicily), Earth Planet. Sci. Lett., 420, 30-44, http://dx.doi.org/10.1016/j.epsl.2015.03.031, 2015.

Plancq, J., Mattioli, E., Henderiks, J., and Grossi, V.: Global shifts in Noelaerhabdaceae assemblages during the late Oligocene-early Miocene, Mar. Micropaleontol., 103, 40-50, http://dx.doi.org/10.1016/j.marmicro.2013.07.004, 2013.

Plancq, J., Mattioli, E., Pittet, B., Baudin, F., Duarte, L. V., Boussaha, M., and Grossi, V.: A calcareous nannofossil and organic geochemical study of marine palaeoenvironmental changes across the Sinemurian/Pliensbachian (early Jurassic, ~ 191 Ma) in Portugal, Palaeogeogr. Palaeoclimatol. Palaeoecol., 449, 1-12, http://dx.doi.org/10.1016/j.palaeo.2016.02.009, 2016.

Plancq, J., Mattioli, E., Pittet, B., Simon, L., and Grossi, V.: Productivity and sea-surface temperature changes recorded during the late Eocene-early Oligocene at DSDP Site 511 (South Atlantic), Palaeogeogr. Palaeoclimatol. Palaeoecol., 407, 34-44, http://dx.doi.org/10.1016/j.palaeo.2014.04.016, 2014.

Prokoph, A., Shields, G. A., and Veizer, J.: Compilation and time-series analysis of a marine carbonate d18O, d13C, 87Sr/86Sr and d34S database through Earth history, Earth Sci. Rev., 87, 113-133, http://dx.doi.org/10.1016/j.earscirev.2007.12.003, 2008.

Riquier, L.: Variations spatio–temporelles des assemblages de nannoplancton calcaire sur un transect palte–forme externe/bassin épicontinental dans le bassin Vocontien (Crétacé inférieur; SE France), Master Thesis, Université Claude Bernard Lyon1, 51 pp, 2002

Reboulet, S., Giraud, F., Colombié, C., and Carpentier, A.: Integrated stratigraphy of the Lower and Middle Cenomanian in a Tethyan section (Blieux, southeast France) and correlations with Boreal basins, Cretac. Res., 40, 170-189, 2013.

Reggiani, L., Mattioli, E., Pittet, B., Duarte, L. V., Veiga de Oliveira, L. C., and Comas-Rengifo, M. J.: Pliensbachian (Early Jurassic) calcareous nannofossils from the Peniche section (Lusitanian Basin, Portugal): A clue for palaeoenvironmental reconstructions, Mar. Micropaleontol., 75, 1-16, 2010.

Reolid, M., Mattioli, E., Nieto, L. M., and Rodriguez-Tovar, F. J.: The Early Toarcian Oceanic Anoxic Event in the External Subbetic (Southiberian Palaeomargin, Westernmost Tethys): Geochemistry, nannofossils and ichnology, Palaeogeogr. Palaeoclimatol. Palaeoecol., 411, 79-94, http://dx.doi.org/10.1016/j.palaeo.2014.06.023, 2014.

Salaviale, C.: Climat, CCD et Nannofossiles Calcaires : Actions et Rétroactions au cours de l'Eocène moyen, Master Thesis, Université Claude Bernard Lyon1, 50 pp, 2013.

Shipboard Scientific Party: Initial Reports of the Deep Sea Drilling Project, edited by: de Graciansky, P. C., Poag, C. W., Cunningham, R. J., Loubere, P., Masson, D. G., Mazzullo, J. M., Montadert, L., Müller, C., Otsuka, K., Reynolds, L., Sigal, J., Snyder, S., Townsend, H. A., Vaos, S. P., and Waples, D., 1985.

Shipboard Scientific Party: Proceedings of the Ocean Drilling Program, Initial Reports, edited by: Erbacher, J., Mosher, D. C., Malone, M. J., Berti, D., Bice, K. L., Bostock, H., Brumsack, H.-J., Danelian, T., Forster, A., and Gladz, C., 2004.

Sprong, J., Youssef, M. A., Bornemann, A., Schulte, P., Steurbaut, E., Stassen, P., Kouwenhoven, T. J., and Speijer, R. P.: A multi-proxy record of the Latest Danian Event at Gebel Qreiya, Eastern Desert, Egypt, J. Micropalaeontol., 30, 167-182, http://dx.doi.org/10.1144/0262-821x10-023, 2011.

Stanley, S. M.: Effects of Global Seawater Chemistry on Biomineralization: Past, Present, and Future, Chem. Rev., 108, 4483-4498, 2008.

Stover, L. E., Brinkhuis, H., Damassa, S. P., de Verteuil, L., Helby, R. J., Monteil, E., Partridge, A. D., Powell, A. J., Riding, J. B., Smelror, M., and Williams, G. L.: Mesozoic-Tertiary dinoflagellates, acritarchs and prasinophytes, edited by: Jansonius, J., and McGregor, D. C., Palynology: Principles and Applications, American Association of Stratigraphic Palynologists Foundation, 2, 641–750, 1996.

Suan, G., Pittet, B., Bour, I., Mattioli, E., Duarte, L. V., and Mailliot, S.: Duration of the Early Toarcian carbon isotope excursion deduced from spectral analysis: Consequence for its possible causes, Earth Planet. Sci. Lett., 267, 666-679, 2008.

Suchéras-Marx, B., Giraud, F., Fernandez, V., Pittet, B., Lécuyer, C., Olivero, D., and Mattioli, E.: Duration of the Early Bajocian and the associated $\delta^{13}C$ positive excursion based on cyclostratigraphy, J. Geol. Soc. London, 170, 107-118, 2013.

Suchéras-Marx, B., Giraud, F., Mattioli, E., Gally, Y., Barbarin, N., and Beaufort, L.: Middle Jurassic coccolith fluxes: A novel approach by automated quantification, Mar. Micropaleontol., 111, 15-25, http://dx.doi.org/10.1016/j.marmicro.2014.06.002, 2014.

Suchéras-Marx, B., Guihou, A., Giraud, F., Lécuyer, C., Allemand, P., Pittet, B., and Mattioli, E.: Impact of the Middle Jurassic diversification of *Watznaueria* (coccolith-bearing algae) on the carbon cycle and $\delta^{13}C$ of bulk marine carbonates, Glob. Planet. Change, 86-87, 92-100, 2012.

Voigt, S., Erbacher, J., Mutterlose, J., Weiss, W., Westerhold, T., Wiese, F., Wilmsen, M., and Wonik, T.: The Cenomanian – Turonian of the Wunstorf section – (North Germany): global stratigraphic reference section and new orbital time scale for Oceanic Anoxic Event 2, Newsl. Stratigr., 43, 65-89, 2008.

Williams, J. R., and Bralower, T. J.: Nannofossil assemblages, fine fraction stable isotopes, and the palaeoceanography of the Valanginian-Barremian (Early Cretaceous) North Sea Basin, Paleoceanography, 10, 815-839, 1995.

Youssef Ali M (2009) High resolution calcareous nannofossil biostratigraphy and paleoecology across the Latest Danian Event (LDE) in central Eastern Desert, Egypt. *Mar Micropaleontol* 72:111–128.

Youssef Ali, M.: High resolution calcareous nannofossil biostratigraphy and paleoecology across the Latest Danian Event (LDE) in central Eastern Desert, Egypt, Mar. Micropaleontol., 72, 111-128, http://dx.doi.org/10.1016/j.marmicro.2009.03.007, 2009.

Zuzlewski, P.: Interactions entre production carbonatée (nannoplancton calcaire) et fluctuations de la CCD pendant le PETM (Paléocène–Eocène), Master Thesis, Université Claude Bernard Lyon1, 51 pp, 2014.